

# Non-adiabatic dynamic of atmospheric unimolecular photochemical reactions of 4,4-difluoro-crotonaldehyde using TD-DFT and TSH approaches

Pedro J. Castro,<sup>\*a,c</sup> Satoshi Maeda<sup>\*b</sup> and Keiji Morokuma<sup>a</sup>

<sup>a</sup> Fukui Institute for Fundamental Chemistry, Kyoto University, Kyoto 606-8103, Japan.

<sup>b</sup> Department of Chemistry, Faculty of Science, Hokkaido University, Sapporo 060-0810, Japan.

<sup>c</sup> Faculty of Chemistry and Pharmacy, Universidad del Atlántico, Barranquilla 081007, Colombia.

\* [pedrojc7@gmail.com](mailto:pedrojc7@gmail.com) and [smaeda@eis.hokudai.ac.jp](mailto:smaeda@eis.hokudai.ac.jp)

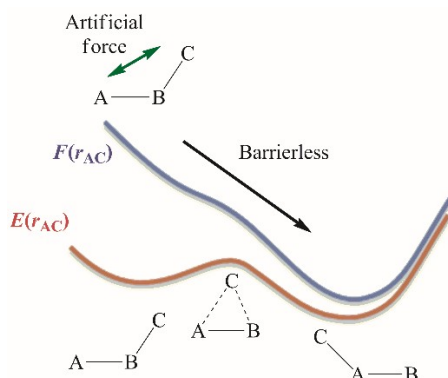


**Figure 1.** Potential energy surface  $E(r_{AC})$  along the  $r_{AC}$  (distance between the atoms A and C), and the AFIR function  $F(r_{AC})$  along the same coordinate (blue).

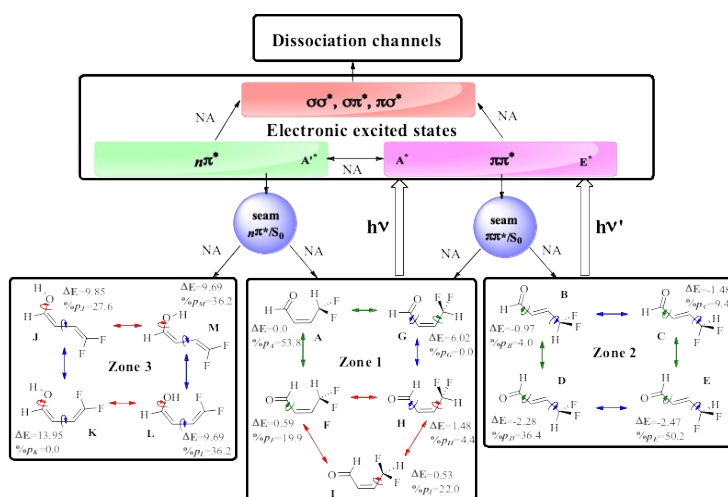


**Figure 2.** Representation of the lower ground state minima and the non-adiabatic processes studied in in this article (NA=non-adiabatic process). Energies (in kcal·mol<sup>-1</sup>) calculated at the B3LYP/6-31G(d) level; % $p_i$  are the Boltzmann population inside each zone expressed in terms of percentage.

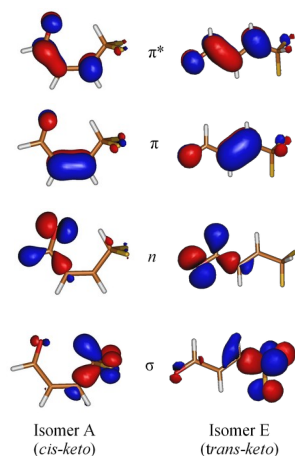


**Figure 3.** Molecular orbitals implied in the single excitations to describe the lower excited states in the A and E isomers.

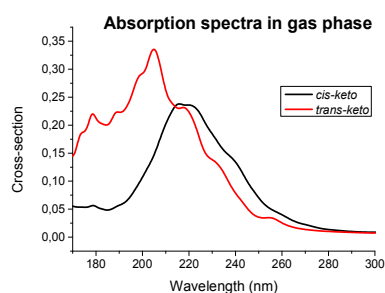


**Figure 4.** Cross-section  $\sigma(E)$  calculated for the *cis* (black line) and *trans-keto* (red line) isomers in the gas phase using a nuclear ensemble composed by 300 geometries and the TD-B3LYP/6-31G(d) level.

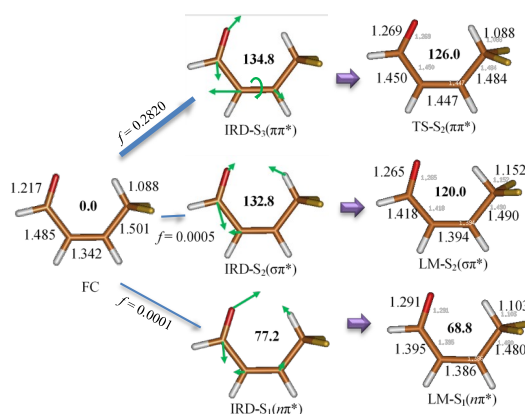


**Figure 5.** Relative energies (kcal·mol<sup>-1</sup>) and bond distances (Å) for FC, TS-S<sub>2</sub>( $\pi\pi^*$ ), LM-S<sub>2</sub>( $\sigma\pi^*$ ) and LM-S<sub>1</sub>( $n\pi^*$ ) calculated at the TD-B3LYP/6-31G(d) level. The oscillator strengths and the representation of the initial relaxation directions (the direction of the force on the corresponding electronic state) are shown at the FC geometry.

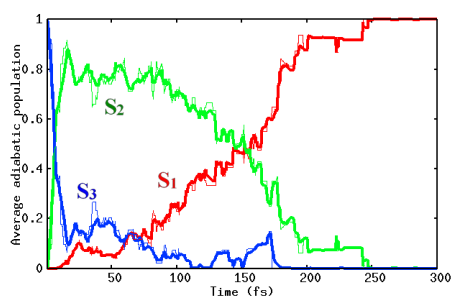


**Figure 6.** Average fraction of trajectories (thin lines) and average adiabatic population (thick lines) from the A isomer for S<sub>1</sub> (red), S<sub>2</sub> (green) and S<sub>3</sub> (blue) as a function of the time (fs).

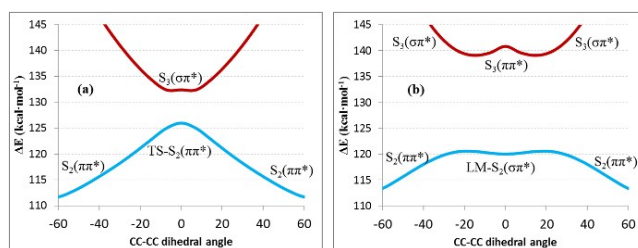


**Figure 7.** Energy profiles ( $\text{kcal}\cdot\text{mol}^{-1}$ ) obtained by the rigid scan along the CC-CC dihedral angle from (a) the  $\text{TS-S}_2(\pi\pi^*)$  and (b) the  $\text{LM-S}_2(\sigma\pi^*)$  calculated at the TD-B3LYP/6-31G(d) level.

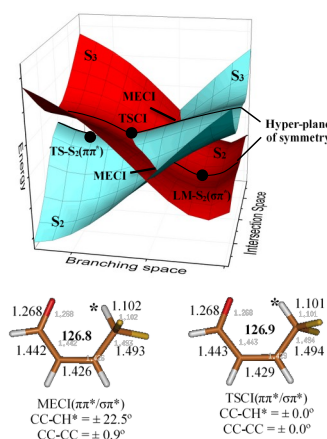


**Figure 8.** Representation of the *seam*( $\pi\pi^*/\sigma\pi^*$ ) respect with the  $\text{TS-S}_2(\pi\pi^*)$  and the  $\text{LM-S}_2(\sigma\pi^*)$ ; energies in  $\text{kcal}\cdot\text{mol}^{-1}$  (bold) and geometries in angstroms and degrees of the MECI and TSCI calculated at the TD-B3LYP/6-31G(d) level.

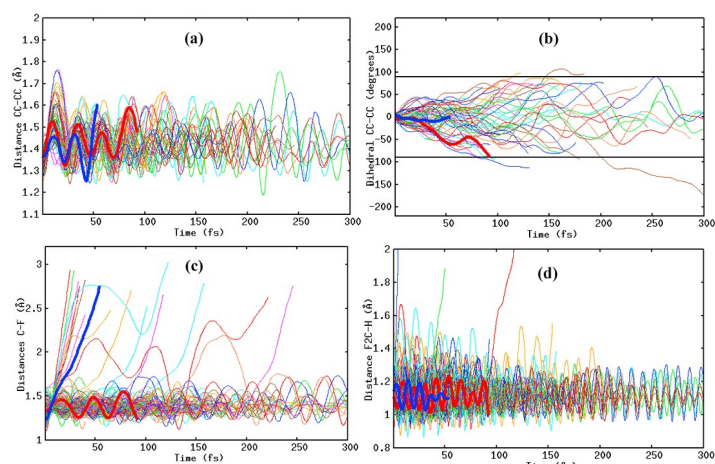


**Figure 9.** Degrees of freedom as a function of the time (fs) starting from the FC zone of the A isomer. The CC-CC distance (a), the CC-CC dihedral angle (b), the C-F distances (c) and the FC-H distance (d). In bold lines are the representative trajectories for the CC-CC *cis-trans* isomerization (red) and the fluorine dissociation (blue).

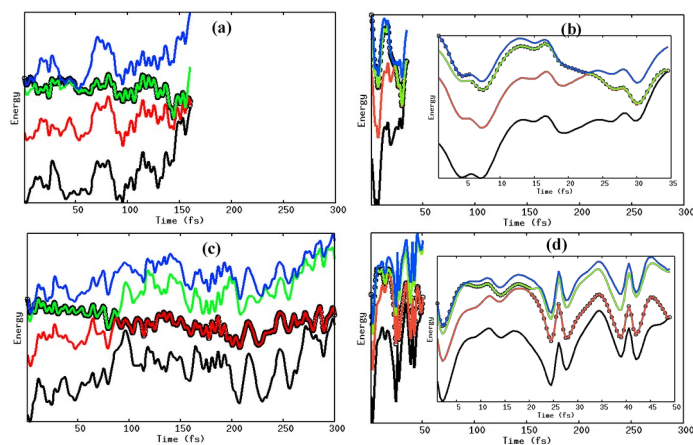


**Figure 10.** Energy of the system as a function of the time (fs) for some typical trajectories along: the CC-CC cis-trans isomerization (a), non-reactive on the  $S_1(n\pi^*)$  state (b), fluorine dissociation (c) and  $\gamma$ -hydrogen abstraction (d). The black, red, green and blue lines represent the  $S_0$ ,  $S_1$ ,  $S_2$  and  $S_3$ , respectively. The black circles highlight the current populated state.

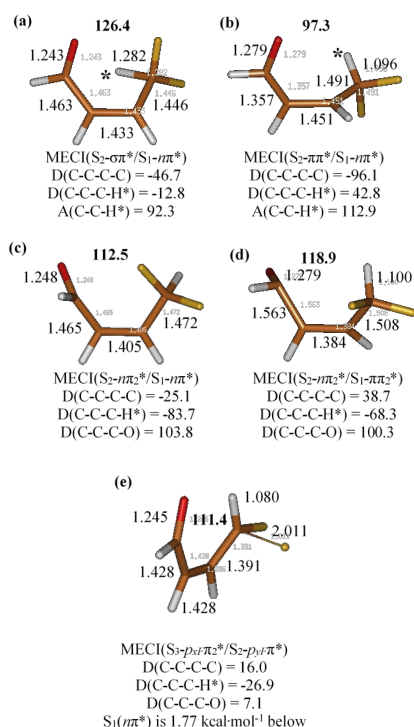


**Figure 11.** Energies in kcal·mol<sup>-1</sup> (bold) and geometries in angstroms and degrees of the MECI( $S_2/S_1$ ) calculated at the TD-B3LYP/6-31G(d) level.

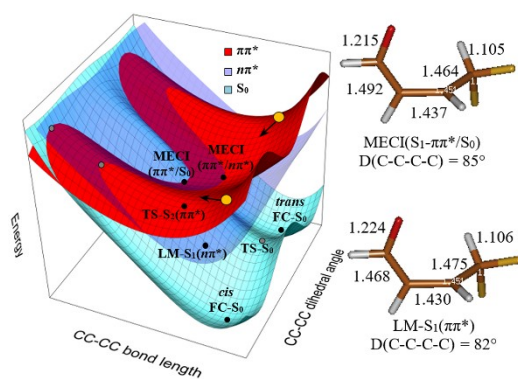


**Figure 12.** Representations of the potential energy surfaces for the  $S_0$ ,  $\pi\pi^*$  and  $n\pi^*$  states along the CC-CC bond distance and the CC-CC dihedral angle. The  $\sigma\pi^*$  state is omitted for simplicity. The arrows show the main component of the gradient for  $\pi\pi^*$  states in the FC geometries.

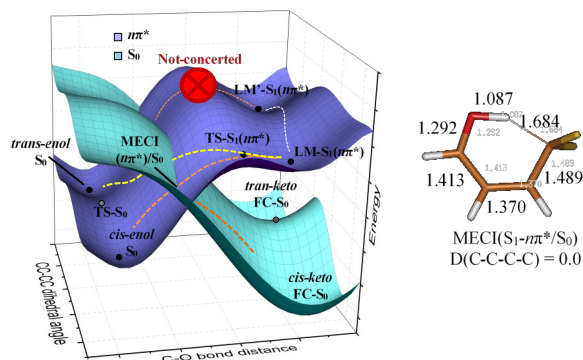


**Figure 13.** Representations of the potential energy surfaces for  $S_0$  and  $n\pi^*$  states along the C-O bond distance and the CC-CC dihedral angle.

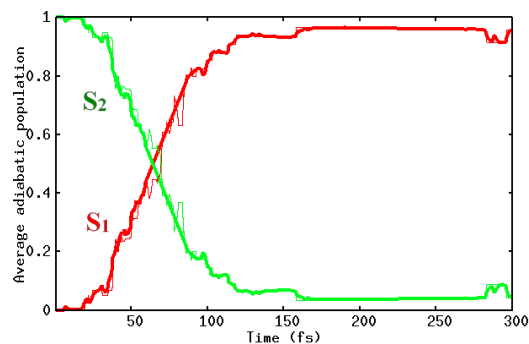


**Figure 14.** Average fraction of trajectories (thin lines) and average adiabatic population (thick lines) from the E isomer for the  $S_1$  (red) and the  $S_2$  (green) as a function of the time (fs).

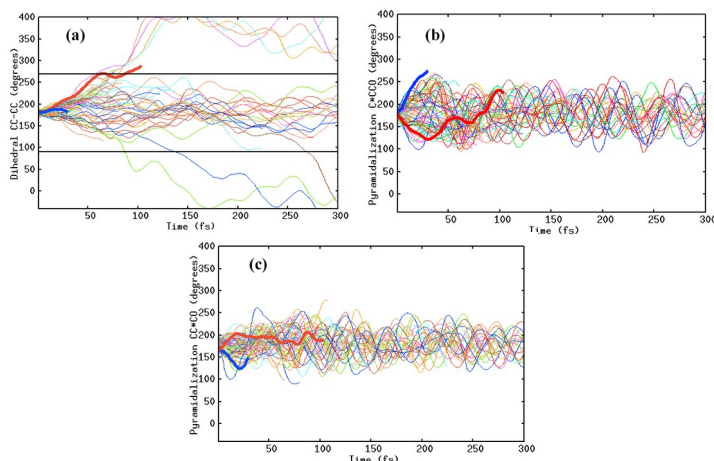


**Figure 15.** Degrees of freedom as a function of the time (fs) starting from the FC zone of the E isomer. The CC-CC dihedral angle (a), the C\*CO pyramidalization (b) and the CC\*CO pyramidalization (c). In bold lines the representative trajectories for the CC-CC *cis-trans* isomerization (red) and the photophysical process (blue).

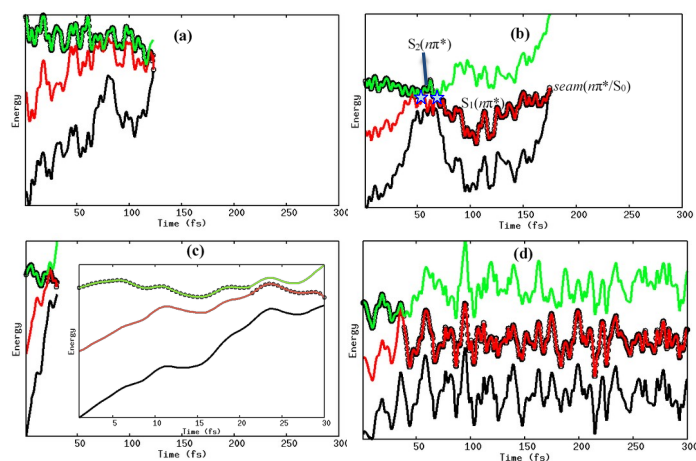


**Figure 16.** Energy of the system as a function of the time (fs) for some typical trajectories along: the CC-CC *trans-cis* isomerization along the  $\pi\pi^*$  state (a), the  $\pi\pi^*$  state (b); a photophysical process (c) and a non-reactive process. The black, red and green lines represent the  $S_0$ ,  $S_1$ , and  $S_2$ , respectively. The black circles highlight the current populated state.